AIP | Applied Physics Letters

Enhanced electron-hole plasma stimulated emission in optically pumped gallium nitride nanopillars

M.-H. Lo, Y.-J. Cheng, H.-C. Kuo, and S.-C. Wang

Citation: Applied Physics Letters **98**, 121101 (2011); doi: 10.1063/1.3570634
View online: http://dx.doi.org/10.1063/1.3570634
View Table of Contents: http://scitation.aip.org/content/aip/journal/apl/98/12?ver=pdfcov
Published by the AIP Publishing

APPLIED PHYSICS LETTERS **98**, 121101 (2011)

Enhanced electron-hole plasma stimulated emission in optically pumped gallium nitride nanopillars

M.-H. Lo,[1,2] Y.-J. Cheng,[1,2,a)] H.-C. Kuo,[2] and S.-C. Wang[2]
[1]*Research Center for Applied Sciences, Academia Sinica, Taipei 11529, Taiwan*
[2]*Department of Photonics and Institute of Electro-Optical Engineering, National Chiao Tung University, 1001 Ta Hsueh Rd., Hsinchu 300, Taiwan*

(Received 9 September 2010; accepted 3 March 2011; published online 21 March 2011)

An enhanced stimulated emission was observed in optically pumped GaN nanopillars. The nanopillars were fabricated from an epitaxial wafer by patterned pillar etching followed by crystalline regrowth. Under optical excitation, a strong redshifted stimulated emission peak emerged from a broad spontaneous emission background. The emission is attributed to the electron-hole plasma gain at high carrier density. The emission slope efficiency was greatly enhanced by 20 times compared with a GaN substrate under the same pumping condition. The enhancement is attributed to the better photon and gain interaction from the multiple scattering of photons among nanopillars. © *2011 American Institute of Physics*. [doi:10.1063/1.3570634]

Gallium nitride has attracted great research interests due to promising applications in UV to blue optoelectronic devices and its strong emission properties. In the past, GaN devices are typically built from epitaxial thin film in a two-dimensional structure. Recently, devices in one-dimensional nanostructure have gained substantial attention for their interesting properties and potential applications.[1–3] The nanodevices, known as nanowires or nanopillars, can be fabricated by self-assembled and selective area growth by molecular beam epitaxy and metalorganic chemical vapor deposition (MOCVD).[4–6] The as-grown nanowires or nanopillars have shown improved material quality, size confinement effect, and significantly enhanced light emission properties.[7–9] Stimulated emission was reported from optically pumped GaN nanowires.[4,10,11]

In this letter, we report the observation of enhanced stimulated emission from GaN nanopillars fabricated by different technique. The nanopillars were fabricated by patterned etching followed by crystalline regrowth from an epitaxial wafer. The nanopillars have an average diameter of 250 nm and a height of 660 nm standing on a GaN substrate. When the sample was optically pumped from the nanopillar end surface by a 355 nm laser with a 37 μm spot size, a strong redshifted stimulated emission peak emerged from a broad spontaneous emission background. The emission peak was redshifted from the spontaneous emission peak by $\sim$5 nm. In previous reports,[4,10,11] redshifts ranging from 5 to above 10 nm were observed, however, without much detail analysis for the underlying mechanism. By analyzing the dependence of redshift on carrier density, we attribute the redshifted emission in our sample to electron-hole plasma gain under high carrier density excitation. The slope efficiency of stimulated emission was greatly enhanced by 20 times compared with that from a GaN thin film substrate under the same pumping condition. We remark that the enhancement is due to better gain and photon interaction enabled by the multiple scattering of photons among nanopillars.

The GaN nanopillar sample was fabricated by self-assembled Ni nanomasked etching and crystalline regrowth from a GaN epitaxial substrate. A 300 nm Si_3N_4 thin film was first deposited on a 3 μm GaN thin film substrate by plasma-enhanced chemical-vapor deposition, followed by subsequent deposition of a Ni thin film by electron-beam evaporation. The sample was subjected to rapid thermal annealing at 850 °C under nitrogen ambiance for 1 min to form self-assembled Ni nanomasks on the Si_3N_4 film surface. Reactive ion etching (RIE) was conducted to etch the Si_3N_4 film using a CF_4/O_2 gas mixture to transfer Ni nanomask pattern down to the Si_3N_4 layer. The sample was subsequently etched down to GaN by an inductive coupled plasma RIE (ICP-RIE) system (SAMCO ICP-RIE 101iPH) operated at 13.5 MHz under a gas mixture of $Cl_2/Ar=50/20$ SCCM for 2 min to form nanopillars. The ICP source power and the bias power of the ICP-RIE system were set at 400 W and 100 W, respectively. The sample was dipped into a nitric acid solution (HNO_3) at 100 °C for 5 min to remove Ni nanomasks. Finally, the etched GaN nanopillars were put back to MOCVD epitaxial regrowth. The Si_3N_4 mask was intentionally left on top of nanopillars to prevent the growth in the vertical direction. Figure 1 is the scanning electron microscope (SEM) plane view image of the fabricated nanopillars. The irregular shape was originated from the self-assembled

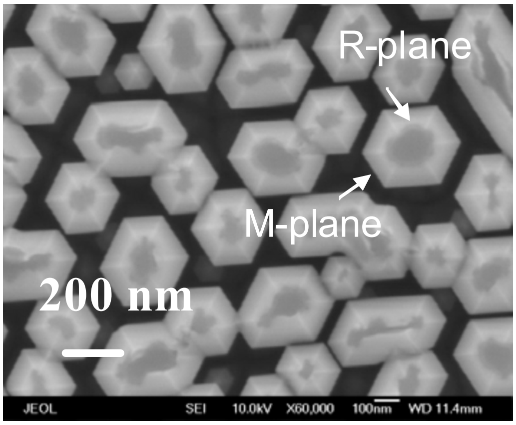

FIG. 1. (a) SEM top view image of fabricated nanopillars, showing M-plane and R-plane crystalline facets.

[a)] Electronic mail: yjcheng@sinica.edu.tw.

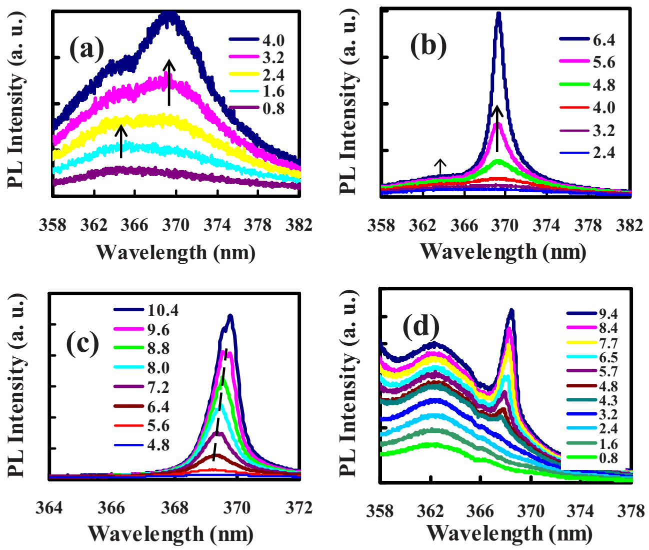

FIG. 2. (Color online) PL spectra of optically pumped nanopillars at (a) below threshold, (b) around threshold, and (c) above threshold. The legends are pump intensity levels in megawatt per centimeter square. (d) PL spectra of GaN thin film substrate.

Ni nanomasks. The regrowth grew additional GaN on the side walls of the etched pillars and formed hexagonal M-plane $\{11\bar{2}0\}$ crystalline facets. It also formed inclined R-plane facets $\{11\bar{2}2\}$ close to the top of nanopillars. The purpose of regrowth was to reduce surface defects created during the ICP-RIE process. The height and the average diameter of nanopillars were 660 nm and 250 nm, respectively.

The nanopillar sample was optically excited by a tripled Nd:YAG 355 nm pulse laser at room temperature. The pulse width was 0.5 ns and the pulse repetition rate was 1 kHz. The laser beam was focused on the sample surface by a 15× UV microscope objective. The nanopillars were pumped from their end surfaces and the pump spot at sample surface had a Gaussian intensity profile with $1/e^2$ diameter of 37 μm. Given the distribution of nanopillars, there were thousands of pillars covered by the pump spot. The photoluminescent (PL) spectrum was collected by the same UV objective and coupled into an optical fiber connected to the input of a spectrometer (Jobin Yvon IHR320) with nitrogen cooled charge-coupled device array.

The PL spectra of nanopillar sample at various pump power intensities are shown in Figs. 2(a)–2(c), where the legends are pump intensity levels in unit megawatt per centimeter square. The pump intensity increases in constant step in all figures. At low pump intensity [0.8 MW/cm^2 curve in Fig. 2(a)], the spontaneous emission spectrum has a maximum around 364.5 nm, which is the nominal emission wavelength of GaN.[12,13] As pump intensity increases, the 364.5 nm spontaneous emission increases in constant increments while an emission peak starting to emerge at around 369 nm. As pump intensity increases further [Fig. 2(b)], the 369 nm peak increases in fast growing (instead of constant) steps. The intensity increase is superlinear and evidently indicates the threshold of stimulated emission. The 364.5 nm spontaneous emission background, in contrast, still increases in constant steps and becomes insignificant compared with the 369 nm peak. Above the threshold [Fig. 2(c)], the 369 nm emission continues to increase in large steps and at the same time slightly redshifts with increasing pump intensity as indicated by the dotted trend line. The 364.5 nm spontaneous emission background becomes totally negligible compared with the emerging 369 nm emission. For comparison, the PL spectra [Fig. 2(d)] of a thin film GaN reference sample from the same epitaxial substrate used to fabricate nanopillar was also measured. At low pump intensity, the PL spectrum has an emission peak around 362.5 nm. The wavelength is shorter than that in nanopillar sample. This variation could be due to strain difference between these two samples from the epitaxial regrowth. As pump intensity increases, a peak emerges at longer wavelength similar to the nanopillar case but with much slower increasing rate. The peak wavelength still slightly redshifts with increasing pump intensity. The stimulated emission of the redshifted emerging peak is less obvious compared with that in the nanopillar sample. It is worth to note the drastic spectral difference between Figs. 2(c) and 2(d). The emerging peak remains comparable to the spontaneous emission peak in the thin film GaN, whereas it is significantly large enough to make spontaneous emission peak totally negligible in the nanopillar sample.

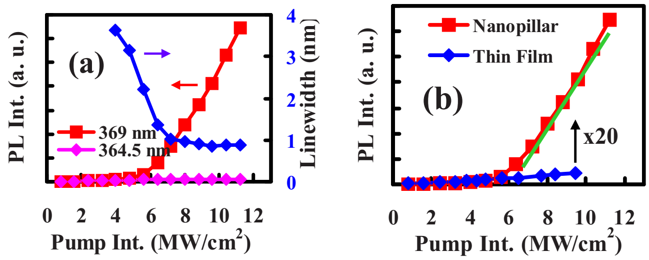

FIG. 3. (Color online) (a) PL intensity of nanopillar at 364.5 nm and 369 nm vs pump intensity, showing the onset of stimulated emission of 369 nm. The linewidth reduces from 4 nm to below 1 nm across threshold. (b) The 369 nm intensity vs pump intensity for the nanopillar and the thin film GaN sample. The slope efficiency of nanopillar is enhanced by 20 times compared with the thin film sample.

To further reveal the stimulated emission threshold of nanopillar sample, the 369 nm peak intensity and its full width at half maximum linewidth versus pump intensity are shown in Fig. 3(a). It clearly shows the onset of 369 nm stimulated emission around pump intensity at 5.5 MW/cm^2. The linewidth substantially decreases from 3.6 to 1 nm across the threshold. The 364.5 nm spontaneous emission peak intensity is also included for reference, which has only a very modest linear increase through out the pump range. The 369 nm peak intensities versus pump intensities for nanopillar and reference sample are shown in Fig. 3(b). The stimulated emission slope efficiency in the regrown nanopillar sample is greatly enhanced by 20 times compared with that in the reference sample. We remark that this large enhancement is due to the better carrier confinement provided by the nanopillar structure and the increase in photon sojourn time due to the multiple scattering among nanopillars. As a result, there is a stronger gain and photon interaction and the stimulated emission efficiency is greatly enhanced. This is in contrast to the bulk GaN material where there is no lateral confinement to enhance gain and photon interaction.

We remark that the gain mechanism of this emerging peak is due to electron-hole plasma at high carrier density. Given the absorption coefficient of GaN 1×10^5 cm^{-1} and radiative carrier recombination coefficient 1.3×10^{-8} cm^3 s^{-1} from reported studies,[14,15] the optically excited carrier density in the center region of Gaussian pump

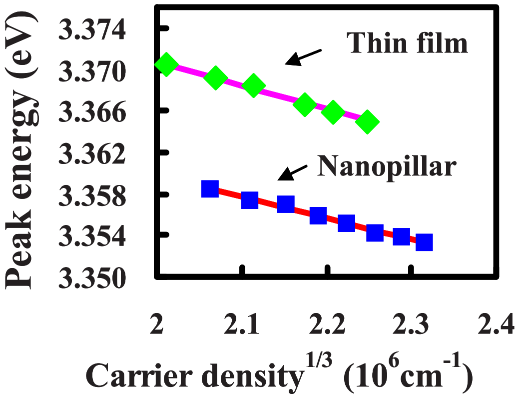

FIG. 4. (Color online) The redshifted peak energies of nanopillar and thin film GaN vs cubic root of excited carrier density. The straight lines are least square fittings.

spot at threshold pump intensity 5.6 MW/cm^2 is about 8.7×10^{18} cm^{-3}. This is in the range of typical reported Mott transition density 10^{18-19} cm^{-3}.[16] Above this critical density, electron-hole plasma is the major gain mechanism.[17,18] A symptomatic behavior of electron-hole plasma emission is the linear redshift with the cubic root of carrier density, which can be predicted by band-gap renormalization calculation. It describes the lowering of transition energy $E_t = E_g - \alpha n^{1/3}$ at above Mott carrier density, where E_g is the band gap transition energy, n is the carrier density, and α is the renormalization coefficient. The observed redshift in emerging peak energy versus the cubic root of the excited carrier density of the nanopillar sample is shown in Fig. 4. The least square fitting line of the above equation to the experimental data is also included, which gives fitted parameters $E_g = 3.40$ eV and $\alpha = 20 \times 10^{-8}$ eV cm. The fitted energy corresponds to 364.66 nm, which is in very good agreement with the observed spontaneous emission peak 364.5 nm [0.8 MW/cm^2 curve in Fig. 2(a)]. The fitted renormalization factor α is also in close agreement with the previous reported experimental values 2.13×10^{-8} to 2.43×10^{-8} eV cm.[19,20] The same fitting is also done for the reference thin film GaN sample, as also shown in Fig. 4. The fitted values are $E_g = 3.417$ eV and $\alpha = 23 \times 10^{-8}$ eV cm. The fitted energy corresponds to peak wavelength of 362.9 nm, again in close agreement with the observed spontaneous emission peak 362.5 nm in Fig. 2(d). The fitted renormalization factor α is also within the range of the previous reported values. From these fitting analyses, we therefore attribute the gain mechanism of emerging peak to electron-hole plasma.

In summary, we have fabricated GaN nanopillars from an epitaxial substrate by patterned etching followed by crystalline regrowth. We observed a large stimulated emission enhancement from the nanopillar sample when it was pumped by a 355 nm pulsed laser. The gain mechanism for the stimulated emission is attributed to electron-hole plasma. The stimulated emission efficiency is greatly enhanced by 20 times compared to that from a GaN thin film substrate under the same pumping condition. We remark that this is due to better gain and photon interaction provided by nanopillar structure.

This work was financially supported by the National Science Council of Taiwan under Contract No. NSC NSC97-2112-M-001-027-MY3 and Academia Sinica Nano-program.

[1] F. Qian, S. Gradečak, Y. Li, C.-Y. Wen, and C. M. Lieber, Nano Lett. **5**, 2287 (2005).
[2] R. Chen, H. D. Sun, T. Wang, K. N. Hui, and H. W. Choi, Appl. Phys. Lett. **96**, 241101 (2010).
[3] H. Sekiguchi, K. Kishino, and A. Kikuchi, Appl. Phys. Lett. **96**, 231104 (2010).
[4] A. Kikuchi, K. Yamano, M. Tada, and K. Kishino, Phys. Status Solidi B **241**, 2754 (2004).
[5] S. D. Hersee, X. Sun, and X. Wang, Nano Lett. **6**, 1808 (2006).
[6] L. W. Tu, C. L. Hsiao, T. W. Chi, I. Lo, and K. Y. Hsieh, Appl. Phys. Lett. **82**, 1601 (2003).
[7] H. Sekiguchi, T. Nakazato, A. Kikuchi, and K. Kishino, J. Cryst. Growth **300**, 259 (2007).
[8] Y. Sun, Y.-H. Cho, H.-M. Kim, and T. W. Kang, Appl. Phys. Lett. **87**, 093115 (2005).
[9] Y. Kawakami, S. Suzuki, A. Kaneta, M. Funato, A. Kikuchi, and K. Kishino, Appl. Phys. Lett. **89**, 163124 (2006).
[10] J. C. Johnson, H.-J. Choi, K. P. Knutsen, R. D. Schaller, P. D. Yang, and R. J. Saykally, Nature Mater. **1**, 106 (2002).
[11] S. Gradečak, F. Qian, Y. Li, H.-G. Park, and C. M. Liebera, Appl. Phys. Lett. **87**, 173111 (2005).
[12] S. Shokhovets, K. Köhler, O. Ambacher, and G. Gobsch, Phys. Rev. B **79**, 045201 (2009).
[13] A. J. Fischer, W. Shan, J. J. Song, Y. C. Chang, R. Horning, and B. Goldenberg, Appl. Phys. Lett. **71**, 1981 (1997).
[14] J. F. Muth, J. H. Lee, I. K. Smagin, R. M. Kolbas, H. C. Casey, B. P. Keller, U. K. Mishra, and S. P. DenBaars, Appl. Phys. Lett. **71**, 2572 (1997).
[15] F. Binet, J. Y. Duboz, E. Rosencher, F. Scholz, and V. Harle, Appl. Phys. Lett. **69**, 1202 (1996).
[16] F. Binet, J. Y. Duboz, J. Off, and F. Scholz, Phys. Rev. B **60**, 4715 (1999).
[17] S. Bidnyk, T. J. Schmidt, B. D. Little, and J. J. Song, Appl. Phys. Lett. **74**, 1 (1999).
[18] K. Kazlauskas, G. Tamulaitis, A. Žukauskas, T. Suski, P. Perlin, M. Leszczynski, P. Prystawko, and I. Grzegory, Phys. Rev. B **69**, 245316 (2004).
[19] X. Zhang, S. J. Chua, W. Liu, and K. B. Chong, Appl. Phys. Lett. **72**, 1890 (1998).
[20] B. K. Meyer, D. Volm, A. Graber, H. C. Alt, T. Detchprohm, A. Amano, and I. Akasaki, Solid State Commun. **95**, 597 (1995).